Bionanotechnology

International Edition: DOI: 10.1002/anie.201411386
German Edition: DOI: 10.1002/ange.201411386

Photothermally Induced Local Dissociation of Collagens for Harvesting of Cell Sheets**

*Jae Dong Kim, June Seok Heo, Teahoon Park, Chihyun Park, Hyun Ok Kim, and Eunkyoung Kim**

Abstract: *The local heating of poly(3,4-ethylenedioxythiophene) (PEDOT) by a photothermal effect directed by near-infrared (NIR) light induces unfolding of absorbed collagen triple helices, yielding soluble collagen single-helical structures. This dissociation of collagens allowed the harvesting of a living idiomorphic cell sheet, achieved upon irradiation with NIR light ($\lambda = 808$ nm). The PEDOT layer was patterned and cells were successfully cultured on the patterned substrate. Cell sheets of various shapes mirroring the PEDOT pattern could be detached after a few minutes of irradiation with NIR light. The PEDOT patterns guided not only the entire shape of the cell sheets but also the spreading direction of the cells in the sheets. This photothermally induced dissociation of collagen provided a fast non-invasive harvesting method and tailor-made cell-sheet patterns.*

Collagen, which has a triple-helical structure, is the one of the most important proteins in cell science.[1–4] Each triple helix is stabilized by numerous hydrogen bonds and supports cell binding. However, the triple helix of collagens unfolds upon heating.[5] Therefore, controlling the dissociation of collagen could be highly important for cell-to-surface interactions and eventually for the detachment of cells. Most cell-detachment studies are undertaken using temperature-responsive culture dishes on which thermoresponsive polymers, such as poly(*N*-isopropylacrylamide) (pNIPAAm), are covalently grafted.[6–10] Although this is one of the most promising methods and is well-established, spatial control of dissociation is particularly difficult using these thermoresponsive substrates. Near-IR (NIR) laser irradiation is "biologically friendly" and can be employed to provide a unique method to spatially control cell behavior.[11–14] By spatially dissociating collagens through the photothermal effect, we now describe, for the first time, tunable cell-sheet detachment and harvesting from a poly(3,4-ethylenedioxythiophene) (PEDOT) substrate without a change in the cell morphology.

PEDOT was directly coated onto polystyrene by polymer solution casting to form SP–PEDOT (PEDOT made by solution casting polymerization (SP)). Then collagen type I (0.3 wt%) was dropcast onto the SP–PEDOT substrate. The thickness of the collagen layer was 14–18 μm, as determined using an Alpha-Step surface profiler. Fibroblasts were seeded on top of a collagen-coated PEDOT substrate (CSP–PEDOT) at a concentration of 3×10^5 cells/dish and were cultured for 3 days. The CSP–PEDOT was irradiated with a NIR diode laser ($\lambda = 808$ nm), with an input power density (I_{pw}) between 1.9 W cm^{-2} and 2.5 W cm^{-2} (see Table S1 in the Supporting Information). When exposed to NIR light, the temperature of the CSP–PEDOT was increased to 41.4 °C (Figure S1). After 5 min of irradiation, the cell sheets were detached from the substrate (Figure 1a). The harvested cell sheets showed positive E-cadherin expression (Figure 1b), verifying that cell–cell interactions are maintained in the harvested cell sheet. Additionally, the cell viability of the harvested sheet was more than 90% (Figure 1c). The efficiency (ε_d) of cell detachment, defined as the ratio of the cell-detached area of the surface divided by the NIR-exposed area, was dependent on the NIR dose (Figures 1d,e). The cell-detached area was always larger than the NIR-exposed area, possibly as a result of a relatively strong cell–cell interactions. Thus ε_d values were 120% and 168%, for I_{pw} values of 1.9 W cm^{-2} and 2.5 W cm^{-2}, respectively (Table S1). The ε_d value was further increased by the increase in the diameter of the NIR-exposed area (d_{NIR}). The diameter of the harvested cell sheet (d_{HCS}) was smaller than d_{NIR}, with d_{HCS} values of 2.3 mm and 4.7 mm when d_{NIR} measured 5 mm and 10 mm, respectively. Nonetheless, the fibrous morphology of the detached cell sheet was the same as that of the cell in the unexposed area, indicating that the detached cell is alive and can retain normal cellular function.[15,16]

As the spatial organization of cells is critical to generate functional tissues, we set out to harvest cell sheets with various shapes. Figure 2a–c show different CSP–PEDOT patterns on the polystyrene substrate. Surprisingly, the patterns guided the adhesion and proliferation of cells, so that cells were observed only at the CSP–PEDOT region (Figure 2d–f) and spread on the surface depending on the pattern shape. Cells were spread omnidirectionally on the circular pattern (Figure 2g). On the other hand, cells were spread along the edge of the square and triangular patterns (Figure 2h,i). This indicates that cell morphology could be controlled by the pattern. After cell culturing for 3 days, the substrate with the cell patterns was irradiated for 5 min with

[*] J. D. Kim, T. H. Park, C. H. Park, Prof. E. K. Kim
Active Polymer Center for Pattern Integration and Department of Chemical and Biomolecular Engineering
Yonsei University, Yonsei-ro 50
Seodaemun-gu, Seoul 120-749 (Republic of Korea)
E-mail: eunkim@yonsei.ac.kr
J. S. Heo, Prof. H. O. Kim
Cell Therapy Center and Department of Laboratory Medicine
Severance Hospital and Yonsei University College of Medicine
Yonsei-ro 50, Seodaemun-gu, Seoul 120-749 (Republic of Korea)

[**] This work was supported by the National Research Foundation of Korea (NRF) grant funded by the Korea government (MSIP) (No. 2007-0056091).

Supporting information for this article is available on the WWW under http://dx.doi.org/10.1002/anie.201411386.

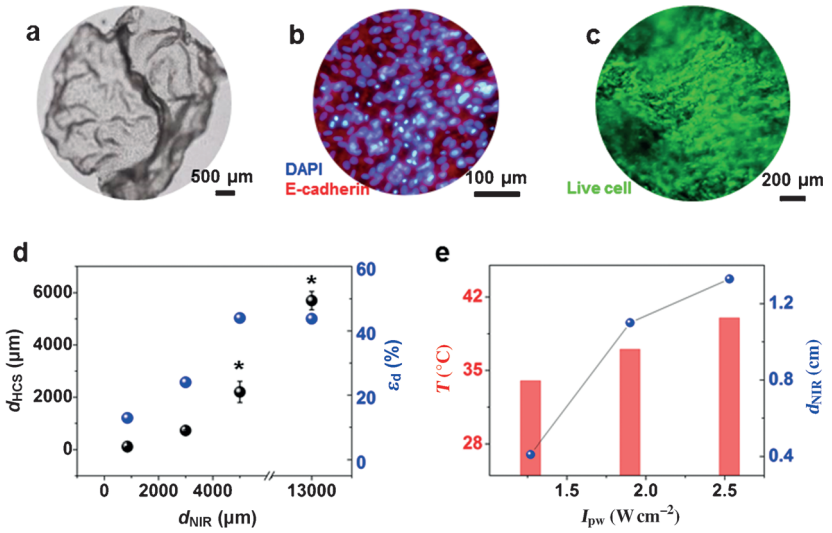

Figure 1. Conditions of cell-sheet formation on the CSP–PEDOT substrates. a) Microscope image of the cell sheet harvested from a circular area. b) Immunofluorescence image of E-cadherin (red) for the interconnected cells in the detached cell sheet. c) Fluorescence image of the detached cell sheet using a live/dead assay. d) Effect of the d_{NIR} value on d_{HCS} (black) and the efficiency of cell detachment ε_d (blue). e) Effect of the I_{pw} value (black) on the temperature increase of the PEDOT surface (red) and on the d_{NIR} value (blue).

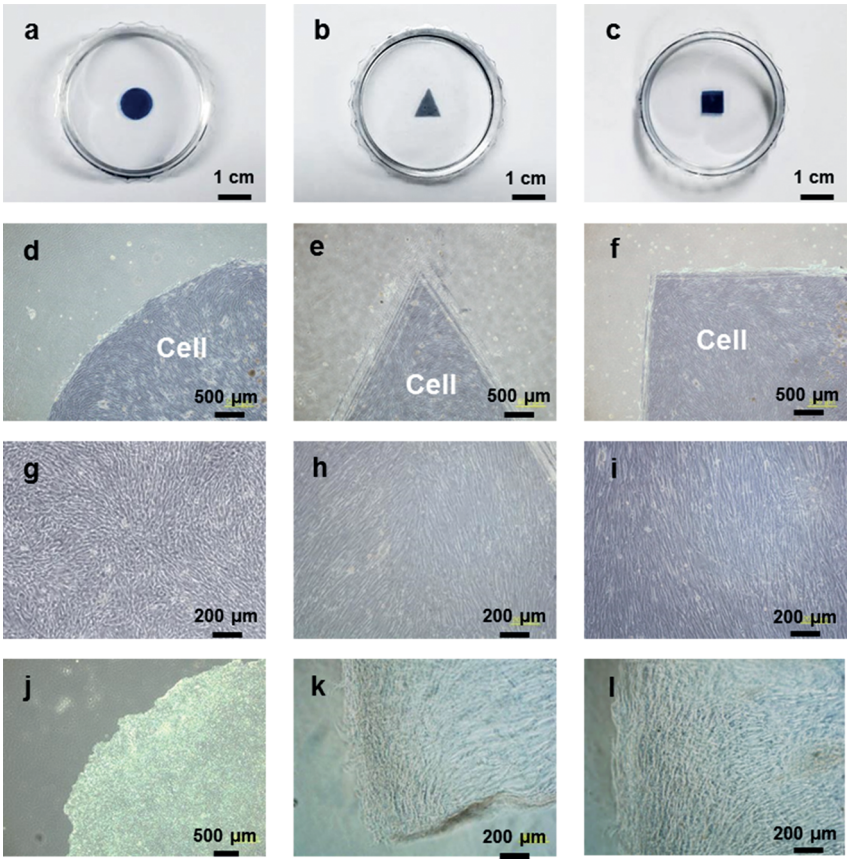

Figure 2. Microscopic images for patterned cell sheets on the various CSP–PEDOT patterns. a–c) Photographs of circular (diameter = 8 mm), triangular (length = 7 mm), and square (length = 5 mm) SP–PEDOT patterns. d–f) Microscopy images showing the cells at the edge of the CSP–PEDOT substrates in (a–c) after culturing for three days. g–i) Microscopy images showing enlarged portions of (d–f) demonstrating the cell morphology on each substrate. j, k) Harvested cell sheets after transfer onto a new polystyrene substrate from (a) and (c), respectively. l) Image showing enlarged portion of (k).

a NIR laser (2.5 W cm^{-2}), to give a patterned cell sheet (Figure 2j,k). The harvested cells were transferred onto a new polystyrene substrate and were found to retain their original patterns even one day after detachment. Figure 2k shows the intact edge of a square-shaped cell sheet on a polystyrene substrate. The morphology of the detached cells appeared as an aligned fibrous shape along the edge of the square pattern (Figure 2l), which is similar to that of the proliferated cells (Figure 2i). In this way, we could harvest cell sheets of different shapes, for the first time, by the NIR-induced method. Compared to the complex and elaborate preparation of pNIPAAm-coated substrates,[15–20] the CSP–PEDOT substrate for cell culture was prepared by simple polymer solution casting, which allows us to control the film properties easily as well as to coat the functional polymer film onto a large-area substrate with various shape.

As the photothermal effect by NIR irradiation occurs on the SP–PEDOT surface and the thermal conductivity of PEDOT is generally very low (0.37 W m^{-1} K^{-1}),[21] the photothermal effect heats mainly the PEDOT surface not the cell media. In this way, heating is localized on the CSP–PEDOT and can warm the adsorbed collagen molecules. It is well-established that cells adhere to the surface through integrins which are receptors that are the bridges for cell–collagen interactions. These interactions are highly sensitive to temperature changes in a cell media.[22,23] Therefore, structural changes in the adsorbed collagens could modulate cell detachment. Cell morphology was not changed greatly by exposure to NIR light (Figure S2a,b), however vacant borders (white regions) were observed around cells on the irradiated region (Figure S2c,d). The cells with vacant borders were detached from the CSP–PEDOT (Figure S2e,f). The scanning electron microscopy (SEM) image of a pristine SP–PEDOT surface showed a rough and porous morphology (Figure S3a). The atomic force microscopy (AFM) image of the pristine SP–PEDOT surface showed a similar rough and porous morphology as in the SEM image (Figure 3a). After treatment with collagen, the rough SP–PEDOT surface was coated with collagen and the surface became more homogeneous as the content of collagen was increased (Figure S3b–e), with the

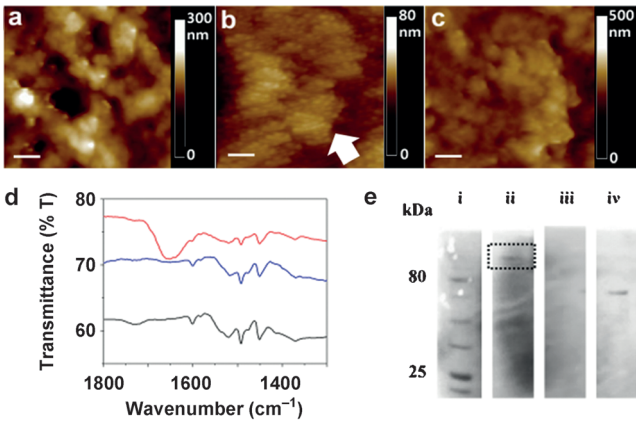

Figure 3. Collagen dissociation at the CSP–PEDOT substrate by a NIR-induced photothermal effect. AFM images for a) pristine SP–PEDOT, and b) CSP–PEDOT, and c) SP–PEDOT coated with collagen (indicated by the white arrow) after exposure to NIR light. Scale bars in (a–c) = 200 nm. d) FTIR spectra for the pristine (black), collagen-adsorbed (red), and NIR-exposed collagen-adsorbed (blue) SP–PEDOT. e) SDS-PAGE analysis of supernatants of samples soaked in 1x phosphate-buffered saline (PBS) solution upon NIR-light exposure: i) protein marker (standard); ii) pristine acid-soluble collagen (control); iii) CSP–PEDOT, and iv) CSP–PEDOT after NIR irradiation for 5 min.

SEM image for a collagen concentration of 0.3 wt % showing a very smooth and homogeneous surface. The AFM image of the CSP–PEDOT substrate also shows a smooth surface (Figure 3b). The surface roughness of the bare SP–PEDOT was 45.8 nm, but that of the collagen-coated SP–PEDOT (collagen at 0.3 wt %) was 3.6 nm. Surprisingly, the SEM image (Figure S3) of the CSP–PEDOT after NIR exposure showed a rough and porous surface, similar to that of the pristine SP–PEDOT. Additionally, very few collagen molecules were observed in the irradiated region, and the surface roughness of this sample was increased to 26.8 nm (Figure 3c, Figure S3f). Collagen molecules have an amide I structure in triple-helical polypeptides, which show characteristic vibrational frequencies for C=O (1655 cm^{-1}) and N–H stretching (3282 cm^{-1}).[24] The FTIR spectrum of the collagen-coated SP–PEDOT showed a C=O stretching band at 1652 cm^{-1} and an N–H stretching band at 3225 cm^{-1} (Figure 3d, Figure S4). After NIR exposure, the spectrum of the surface showed no amide I peaks and it was similar to the spectrum obtained for the pristine SP–PEDOT. This similarity indicates that the collagens adsorbed onto the SP–PEDOT surface, before NIR exposure, had dissociated from the surface upon NIR exposure. This may generate the aforementioned vacant borders around the cells on the NIR-irradiated surfaces.

To analyze the molecules which has dissociated from the surface, a cell-media supernatant was collected from the CSP–PEDOT after cell-sheet detachment and was analyzed using SDS-PAGE analysis. In a control solution, collagens were dissolved in acidic solution, which showed characteristic bands for triple-helical folded collagens (see the dotted square in Figure 3e, lane ii; $M_w = 300$ kDa, as referenced to lane i). No dissolved collagens were detected from the cell media supernatant of the unexposed SP–PEDOT (Figure 3e, lane iii), as collagens were well adsorbed onto the SP–PEDOT surface, providing strong connections between the cells and the substrate. On the other hand, a new band appeared in a low molecular weight region ($M_w \approx 100$ kDa) from the supernatant of the NIR-exposed CSP–PEDOT (Figure 3e, lane iv). This indicates that the triple-helical folded collagens were transformed into unfolded soluble single helices in the NIR-exposed area. It has been established that the stability of collagen triple helices is dependent on the interaction between collagens and water, which is influenced by pH or heat.[25] For example, the water content in collagen molecules decreases as temperature is increased from 25 to 40 °C.[26] The decrease of the water content in collagens at higher temperature may change the interactions within the triple helices and induce dissociation of the collagen assembly,[27,28] leading to the unfolding of the triple helices into a polypeptide chain in a random-coil configuration. The unfolded collagens have a greater affinity for water than the triple helices. This collagen unfolding process could be related to the dissociation of the proteins.[29,30] As the temperature of the SP–PEDOT film was increased by the photothermal effect, only in the area exposed to light is the cell sheet detached. This is attributed to a photothermal effect where the temperature increases only locally on the film surface, not throughout the entire cell media. Indeed, the average temperature of the medium was 31.4 °C, whereas that of the CSP–PEDOT was 41.4 °C. Upon local heating at the surface, the water molecules near the surface are also heated so that water molecules quickly penetrate into the unfolded collagens, possibly forming new hydrogen-bonding interactions with them. The unfolded collagens with single-helical structure have high solubility in aqueous solution and low molecular weights corresponding to one third ($M_w \approx 100$ kDa) of the molecular weight of the triple helices ($M_w \approx 300$ kDa; Figure 3e, lane iv).

Figure 4 describes the detachment mechanism of a cell sheet by local dissociation of collagen on the SP–PEDOT surface. As the collagens with triple-helical structure are converted into soluble hydrated single helices which dissolve and dissociate out into the medium, vacant borders are formed around the cells. The affected cells are no longer connected to the surface through the collagens after NIR exposure. Although cells cultured on a pristine SP–PEDOT substrate and on CSP–PEDOT prepared from the diluted collagen solution (< 0.3 wt %) could be harvested by the NIR method, for SP–PEDOT cell sheets were not obtained because of the poor cell–cell interactions. It indicates that collagens adsorbed on the SP–PEDOT have two functions for the harvesting of cell sheets: 1) to support cell binding on a CSP–PEDOT substrate and 2) to detach cell sheets completely by the dissociation of collagens when the CSP–PEDOT surface is heated by the photothermal effect.

In conclusion, a live cell sheet is harvested by the dissociation of adsorbed collagens on a SP–PEDOT surface using a NIR-radiation-directed photothermal method, leading to a spatially controllable cell-sheet detachment. The photothermal effect of NIR light on CSP–PEDOT films played an important role in the selective dissociation of collagen molecules, allowing the detachment of a patterned cell sheet with intact cell morphology. This new cell-sheet

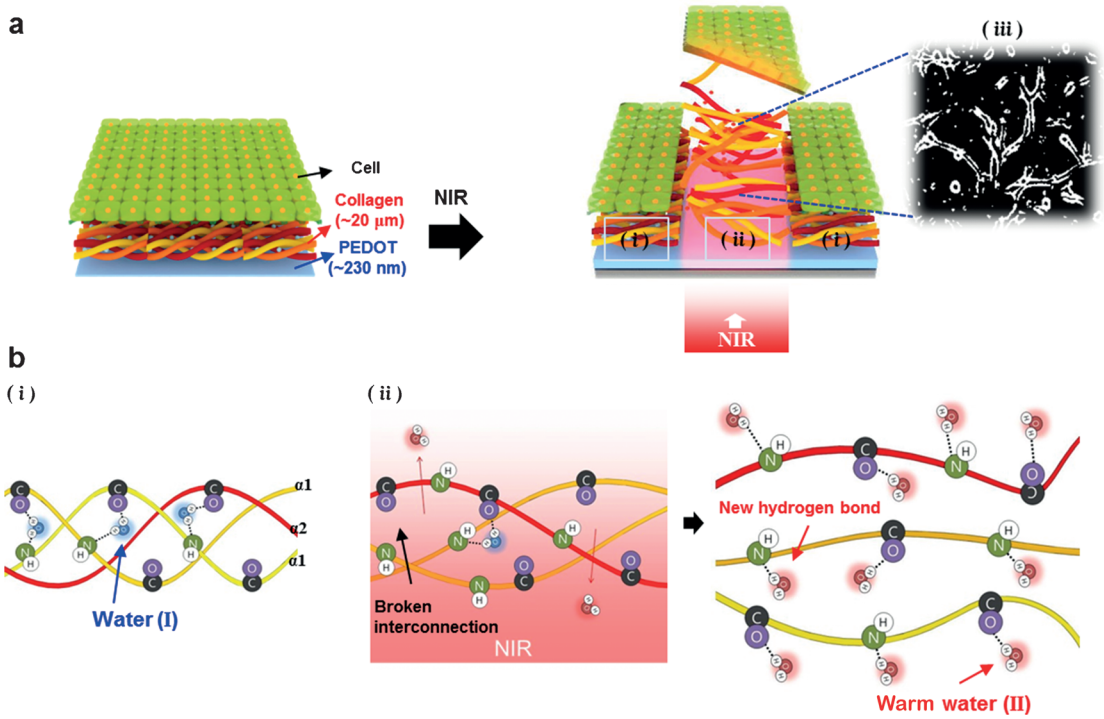

Figure 4. Schematic representation showing the mechanism of photothermal cell detachment from the CSP–PEDOT substrate after exposure to NIR light. a) Adhesion of fibroblasts onto a CSP–PEDOT substrate and detachment of the cell sheets by the heat generated on the surface upon NIR-light exposure (ii), showing vacant borders around cells in region (ii). iii) A microscopy image of region (ii). b) Structure of collagens having one α2 and two α1 polypeptide chains in the unexposed region (i) and dissociated, unfolded collagens in the NIR-exposed region (ii). The water molecules (I) in the triple-helical structure are expelled upon heating of the SP–PEDOT at region (ii) to generate single-helical collagens that form new hydrogen-bonding interactions with warm water molecules (II) and then dissolve into cell media.

harvesting process is quite efficient and may provide useful insights into the study of intercellular interactions and in the development of cell-based sensors and artificially engineered tissues.

Keywords: collagen peptides · conducting materials · photothermal effect · polymers · protein folding

How to cite: *Angew. Chem. Int. Ed.* **2015**, *54*, 5869–5873
Angew. Chem. **2015**, *127*, 5967–5971

[1] C. M. Yamazaki, I. Nakase, H. Endo, S. Kishimoto, Y. Mashiyama, R. Masuda, S. Funtaki, T. Koide, *Angew. Chem. Int. Ed.* **2013**, *52*, 5497–5500; *Angew. Chem.* **2013**, *125*, 5607–5610.
[2] J. Heino, *Bioessays* **2007**, *29*, 1001–1010.
[3] J. T. Parsons, A. R. Horwitz, M. A. Schwartz, *Nat. Rev. Mol. Cell Biol.* **2010**, *11*, 633–643.
[4] D. E. Discher, P. Janmey, Y.-L. Wang, *Science* **2005**, *310*, 1139–1143.
[5] P. H. von Hippel, *J. Am. Chem. Soc.* **1965**, *87*, 1824–1824.
[6] A. K. Kristopher, B. Branimir, T. L. Bruce, M. Milan, *Proc. Natl. Acad. Sci. USA* **2010**, *107*, 4872–4877.
[7] B. Ohlstein, T. Kai, E. Decotto, A. Spradling, *Curr. Opin. Cell Biol.* **2004**, *16*, 693–699.
[8] C. O'Neill, P. Jordan, G. Ireland, *Cell* **1986**, *44*, 489–496.
[9] D. E. Ingber, *Int. J. Dev. Biol.* **2006**, *50*, 255–266.
[10] J. P. Spatz, B. Geiger, *Methods Cell Biol.* **2007**, *83*, 89–111.
[11] T. Sada, T. Fujigaya, Y. Niidome, K. Nakazawa, N. Nakashima, *ACS Nano* **2011**, *5*, 4414–4421.
[12] J. M. You, J. S. Heo, J. H. Kim, T. H. Park, B. G. Kim, H.-S. Kim, Y. J. Choi, H. O. Kim, E. K. Kim, *ACS Nano* **2013**, *7*, 4119–4128.
[13] H. K. Moon, S. H. Lee, H. C. Choi, *ACS Nano* **2009**, *3*, 3707–3713.
[14] S. Thalhammer, G. Lahr, A. Clement-Sengewald, W. M. Heckl, R. Burgemeister, K. Schutze, *Laser Phys.* **2003**, *13*, 681–691.
[15] R. Yoshida, K. Uchida, Y. Kaneko, K. Sakai, A. Kikuchi, Y. Sakurai, T. Okano, *Nature* **1994**, *374*, 240–242.
[16] Y. Kaneko, K. Sakai, A. Kikuchi, Y. Sakurai, T. Okano, *Macromol. Symp.* **1996**, *109*, 41–53.
[17] N. Yamada, T. Okano, H. Sakai, F. Karikusa, Y. Sawasaki, Y. Sakurai, *Makromol. Chem. Rapid Commun.* **1990**, *11*, 571–576.
[18] Y. Akiyama, A. Kikuchi, M. Yamato, T. Okano, *Langmuir* **2004**, *20*, 5506–5511.
[19] T. Okano, N. Yamada, H. Sakai, Y. Sakurai, *J. Biomed. Mater. Res.* **1993**, *27*, 1243–1251.
[20] Z. Tang, Y. Akiyama, M. Yamato, T. Okano, *Biomaterials* **2010**, *31*, 7435–7443.
[21] T. H. Park, C. H. Park, B. G. Kim, H. J. Shin, E. K. Kim, *Energy Environ. Sci.* **2013**, *6*, 788–792.
[22] A. Veis, *The Macromolecular Chemistry of Gelatin*, *Vol. 5*, Academic Press, New York, **1964**, pp. 1–433.
[23] C. Mu, D. Li, W. Lin, Y. Ding, G. Zhang, *Biopolymers* **2007**, *86*, 282–287.
[24] B. de Campos Vidal, M. L. Mello, *Micron* **2011**, *42*, 283–289.
[25] E. Leikina, M. V. Mertts, N. Kuznetsova, S. Leikin, *Proc. Natl. Acad. Sci. USA* **2002**, *99*, 1314–1318.

[26] H. B. Bull, *J. Am. Chem. Soc.* **1944**, *66*, 1499 – 1507.
[27] "Theory and Industrial practice": R. Schreiber, H. Gareis, *Gelatin Handbook*, Wiley-VCH, Weinheim, **2007**, chap. 1, pp. 1 – 347.
[28] R. E. Baier, *Appl. Chem. Protein Interfaces* **1975**, *145*, 1 – 25.
[29] L. Bozec, M. Odlyha, *Biophys. J.* **2011**, *101*, 228 – 236.
[30] B. J. Bennion, V. Daggett, *Proc. Natl. Acad. Sci. USA* **2003**, *100*, 5142 – 5147.

Received: November 26, 2014
Revised: January 20, 2015
Published online: February 25, 2015

